Experimental evaluation of the effect of braking torque on bogie dynamics

M. Dhanasekar*, C. Cole and Y. Handoko

Centre for Railway Engineering,
Central Queensland University, Australia
E-mail: m.dhanasekar@cqu.edu.au
E-mail: c.cole@cqu.edu.au
E-mail: yunendar@inka.web.id
*Corresponding author

Abstract: This paper reports a full-scale laboratory test carried out for the evaluation of the effect of braking torque on bogie dynamics. Precision instruments have been used as the limited length of the track restricted the operating speed to less than 4m/s. It is shown that by judiciously controlling the brake pressure and its application time, the skid of the braked wheelset could be achieved. The instrumented bogie is shown to possess excellent potential for being used as an onboard system for monitoring the dynamics of cash trains during brake application without the need for a wayside magnetic encoder system.

Keywords: experimental methods; instrumented bogies; wayside linear measurement encoder; shaft encoders; accelerometers; brake cylinders; brake normal force; brake tangential force; wheel-rail friction.

Reference to this paper should be made as follows: Dhanasekar, M., Cole, C. and Handoko, Y. (2007) 'Experimental evaluation of the effect of braking torque on bogie dynamics', *Int. J. Heavy Vehicle Systems*, Vol. 14, No. 3, pp.308–330.

Biographical notes: Manicka Dhanasekar is an Associate Professor and Structural Engineer involved in rail research for over 12 years with major focus on wheel-rail contact forces and damage mechanisms of railheads and wheel thread surfaces. He has been the Director of the Centre for Railway Engineering at Central Queensland University since 2001. He has published more than 100 peer-reviewed journal and conference proceedings papers, including invited keynote papers.

Colin Cole is the Deputy Director and Mechanical Group Leader at the Centre for Railway Engineering, at Central Queensland University. He has been involved in rail research in train and vehicle dynamics for 12 years and has rail industry experience dating back to 1984. He has published 28 technical papers, a book chapter and two patents. He is a member of the Engineers Australia and the Railway Technical Society of Australia. His research and professional interests include train and vehicle dynamics, mechanical vibrations, simulation of non-linear systems, neural network systems, fuzzy logic, genetic/evolutionary algorithms, automatic control and industrial hydraulics.

Yunendar Handoko is an Assistant Manager (Commercial and Technical) at the Rolling Stock Division of INKA Indonesia. He received his Bachelor of Mechanical Engineering qualification from ITB, Bandung, in 1995 and completed his PhD studies at the Centre for Railway Engineering, Central Queensland University, Australia in 2006. His research interest includes wagon modelling, simulation and design. He has more than eight papers to his credit.

1 Introduction

The design characteristics of railway bogies are usually assessed from the vertical and lateral dynamic analyses. The effect of longitudinal forces, especially brake torques to bogie dynamics, is seldom studied although the longitudinal forces modify the lateral creep forces at the wheel-rail contact patch. The relationship between creepage and creep forces was first defined by Carter (1926) who was concerned with the action of locomotive wheels when large tangential forces were transmitted during acceleration and braking. The formulation given by Carter was based on two-dimensional analysis of a cylinder rolling on a plane that only considered the force on the rolling direction. Polach (1999) proposed a method that predicted high creepage cases efficiently with significant saving in computational effort relative to other methods (Dukkipati, 2000). Application of this method to wagon dynamics simulation, with particular attention to locomotives running at the adhesion limit, was also reported by Polach (2005) with good agreement between theory and field experiments.

Balas et al. (2001) developed a model for the sliding wheel to assist the study and design of the braking equipment, including the Anti-lock Braking System (ABS). In this model the friction coefficient between the wheel and the rail was considered as a function of the slip of the wheel. Olson (2001) has studied the longitudinal dynamics of ground vehicles that include non-linear wheel braking and acceleration models. Although his work is focused on road vehicles, it is still appropriate to the study of railway wagon braking. In formulating the equations of motion of a wheel under braking condition, Olson considered the slip as a dynamic state variable, replacing the absolute rotational rate of the wheel speed. Lixin and Haitao (2001) studied the dynamic response of wagons in a heavy haul train during braking mode using ADAMS/Rail software that could predict the three dimensional dynamic response of the wagon under braking conditions. From their investigation it was concluded that the application of braking has adversely affected the lateral and vertical dynamic performance of the wagon. However, the investigation was limited to constant brake shoe force although the brake force is normally a function of time; furthermore, the effect of wheel-lock or skid phenomena was not investigated. Berghuvud (2002) investigated the effect of brake force application to keep the speed constant for wagons negotiating curves with no attention paid to the effect of variation in speed to the curving performance. This paper describes an experiment that allows for variations in brake shoe force, the speed and wheelset skid.

2 Experimental design

The primary objective of the test was to examine the dynamics of bogies subjected to brake torque. A three-piece bogie provided by Queensland Rail (QR) was used in the experiment. Due to space limitation in the Heavy Testing Laboratory (HTL), Central Queensland University (CQU), a 24 m long track that restricted the maximum speed of the bogie to 4 m/s was constructed. Brake was applied only to the rear wheelset and the un-braked leading wheelset allowed comparison of the dynamics of the braked and the un-braked wheelsets. The brake force was controlled using a pneumatic circuit that maintained the brake pressure and brake application time (time needed to reach maximum pressure) to the desired levels. A set of precision equipment and devices was installed on the bogie in order to gather data of the applied brake force, the longitudinal, the vertical and the lateral dynamics (travel distance, velocity and acceleration), as well as the wheelset rotation (pitch).

Andrews (1986) reported a similar experiment carried out in the then British Railway Electrical Laboratory, Willesden, with a particular focus on traction effects to locomotive bogie dynamics. A single bogie powered with a traction motor and loaded appropriately to simulate the static axle load was used in their test. Their test did not pay any attention to braking as adhesion and traction torques induced slip were the major study parameters. The test described in this thesis was primarily developed for examining the effect of brake torque to bogie dynamics. No other experiment similar to the one reported in this paper was found in the literature.

The 24 m long track was divided into zones of acceleration, steady-state rolling (coasting) and deceleration, followed by a safety buffer zone as shown in Figure 1. As constant braking rate is most likely not achievable using the available brake equipment, the braking section was chosen longer than ideally necessary. The effect of potential lower deceleration rate on stopping distance is shown by the dashed lines in the speed profile curves of Figure 1.

Figure 1 Track section and estimated speed profile

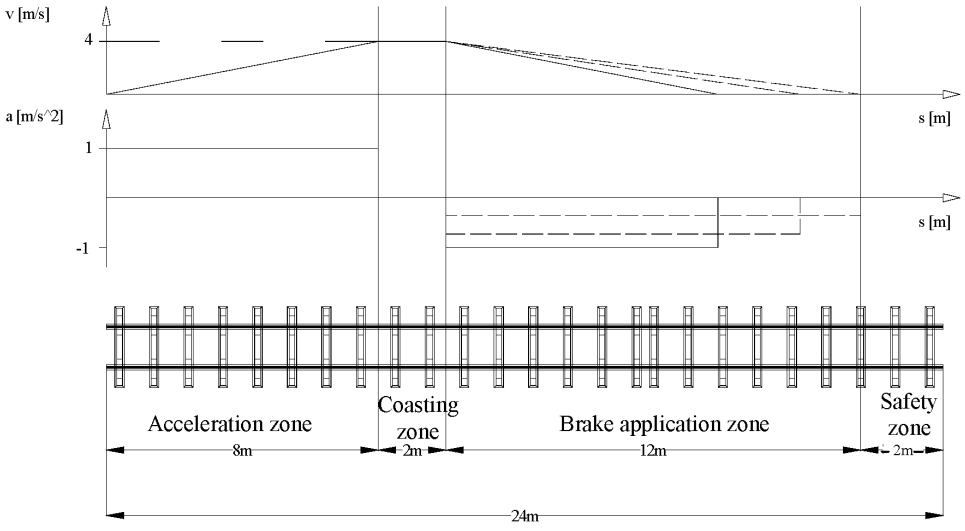

It will be useful to view the experimental design from practical perspective, in particular the brake forces relative to static load. For this purpose brake severity expressed in terms of Brake Force Ratio (BFR = brake shoe normal forces/static axle load) is considered here. In general a fully loaded wagon would be subjected to a BFR of approximately 15% or less and empty wagons up to 45%. In the experiment, we report two cases of brake pressure 130 kPa and 180 kPa that provided maximum brake shoe forces of 4.65 kN and 6.50 kN respectively. As the axle load at only 18 kN (half of one bogie weight), Case #1 (130 kPa) corresponds to BFR of 52% whilst Case #2 (180 kPa) corresponds to 72% as only one axle was braked. The experimental condition should therefore be considered as defining 'severe braking' scenario.

2.1 Braking force

The bogie used in the experiment transmits the brake torque through tangential friction force due to the contact between the brake shoes and the wheel tread. Force on the brake shoes is provided by a cross-beam that is connected to the brake shoes on one side and is attached to the actuators (brake cylinders) though pistons on the other side. The movement of the brake beam is guided by slots provided in the side frame.

Figure 2 shows the forces applied to the system; due to symmetry only half of the system is shown. It is, therefore, very important to measure the forces exerted by the actuator F_{ct1} and F_{ct2} as well as the tangential force F_t produced due to friction between the shoes and the wheels as accurately as possible. By knowing the magnitude of the tangential force produced, the actual torque applied to the wheels can easily be calculated from the geometric data of the wheelset.

Figure 2 Forces acting on brake system of the bogie

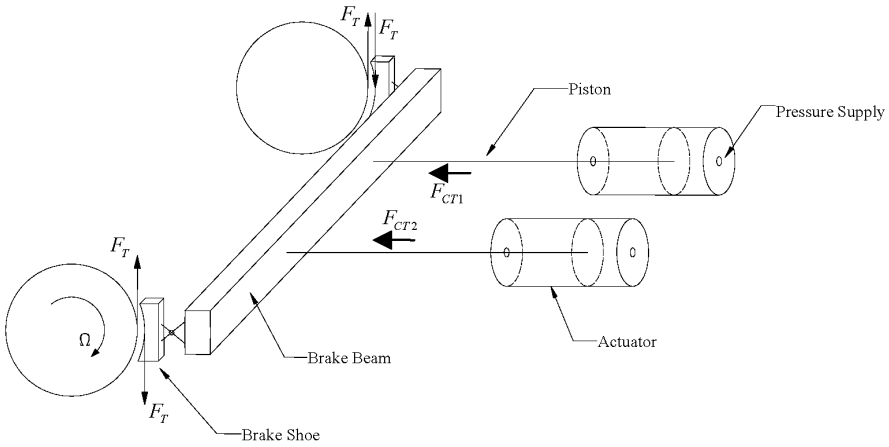

The bogie brake cylinder was capable of supplying air pressure much larger than what was required; as such, during the test the pressure supplied to the brake cylinder was maintained at just sufficient level to produce normal load under 8.2 kN on each wheel. For brake torque calculation, the tangential brake shoe force is required. As the friction coefficient between the brake shoes and the wheels was not precisely known, it was decided to measure the tangential brake shoe force so that both the brake torque and the friction coefficient could be calculated.

2.2 Longitudinal dynamics of the bogie

The longitudinal acceleration, longitudinal velocity, longitudinal travel distance and the wheelset rotation and angular velocity relative to its lateral axis were measured accurately during the test. The brake torque application to the wheel creates longitudinal slip or creepage in the wheel rail contact patch. The longitudinal slip ξ_x is of interest and has been measured indirectly through v_c, the circumferential velocity in the wheel-rail point of contact and v, the longitudinal velocity of the wheel. To predict the longitudinal slip as low as $\xi_x = 0.02$ during braking, for very low speed of 0.1 m/s, the required level of accuracy of the relative velocity measurement device was 0.002 m/s.

Accelerations in all the three directions were measured on each axle box. Assuming permanent vertical connection between the side frame and the axle box allowed the detection of vertical running behaviour and pitch of the side frames of the bogie. By obtaining acceleration data of the axle boxes in all three directions, yaw and lateral motions as well as roll of the wheelset was calculated assuming the set-up was held symmetric to bogie frame. Five accelerometers (a total of ten accelerometers) per wheelset were used in the experiment, which comprised of two each along the vertical and longitudinal axes and one along the lateral axis of the wheelset.

3 Equipment, installation and Data Acquisition (DAQ)

3.1 Brake force measurement: strain gauge

The design of brake beam adversely affected the measurement of the tangential forces. Therefore, the brake beam of the braked wheelset was slitted as shown in Figure 3 and hangers were then used to replace the function of the slots to support and guide the movement of the brake beam. The tangential brake force was measured from the strain in the hanger. Figure 4 shows the strain gauged hanger installation on the bogie. The design of hanger installation assembly allowed accurate positioning of the brake beam relative to wheelset both vertically and laterally.

The force exerted by the brake actuator was measured by fitting a strain gauge in the brake rod as shown in Figure 5.

Figure 3 Modification (cutting) of the brake beam slider

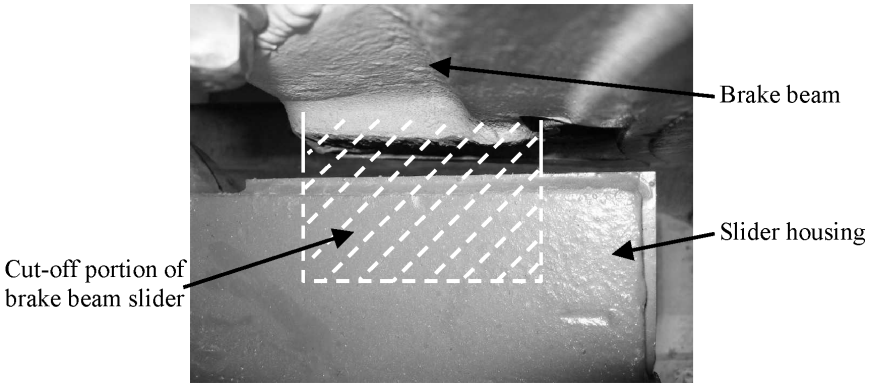

Figure 4 Tangential brake force measurement

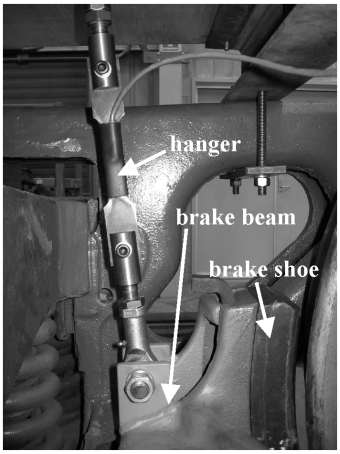

Figure 5 Brake cylinder and brake rod with strain gauge

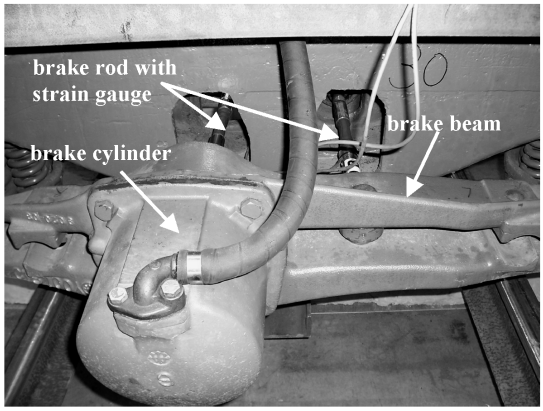

In the non-braked leading wheelset, the movement of the brake beam was restricted by a plate welded onto the slot providing a thread to allow adjustment of the longitudinal clearance using a bolt (Figure 6).

Figure 6 Brake beam stopper of the non-braked wheelset

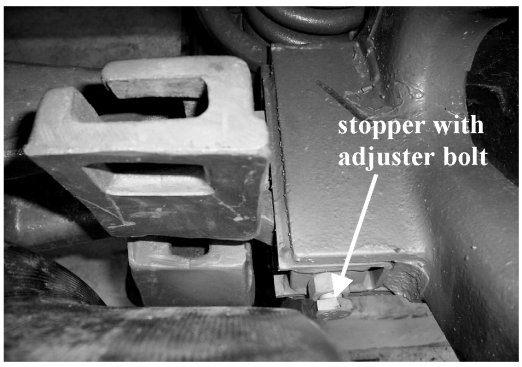

3.2 Longitudinal movement measurement: magnetic linear encoder

A magnetic linear encoder was used as a sensor to measure the longitudinal motion of the bogie, which is capable of accurately detecting incremental reading on a longitudinally installed magnetic tape. The picture of the sensor and the magnetic tape is shown in Figure 7.

Figure 7 The carriage and guide beam for linear encoder

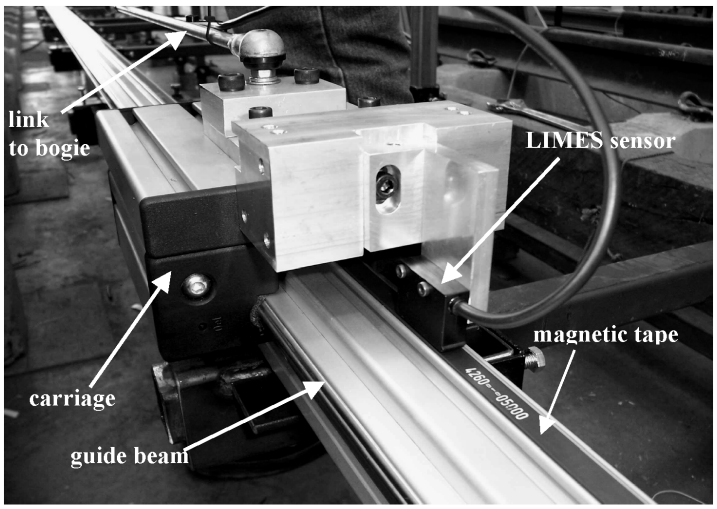

An independent support and guidance system was designed to provide longitudinal support for the magnetic tape which also guided a carriage with the sensor located on it ensuring safe signal reception. A longitudinally rigid and laterally and vertically free-to-move link system was installed between the bogie frame and the carriage. The mounting system of the sensor allowed for the adjustment of the gap between the sensor and the magnetic tape.

3.3 Wheel rotation measurement: shaft encoder

To measure the rotation of both wheelsets, 42 mm hollow shaft encoders of 10,000 pulses per revolution were chosen. Figure 8 shows the installation of the shaft encoder to the axle end of one of the wheelsets. To achieve this installation the axle boxes were required to be cut open to provide access to the fitting of the encoder adaptor. In addition to cut opening, a rigid link was also attached for the installation of the accelerometer box.

Accelerometer measurements

The accelerometers were compactly installed in a small rigid box as shown in Figure 8. The accelerometer signal was filtered by a second order Butterworth filter, cutting off the signal at the frequency of 20 Hz.

Track construction

The test track was carefully constructed to get the satisfactory straight track along the length of 24 m by the professionals from the QR.

Wheel and rail profiles

The railhead and wheel profiles were carefully measured using MINIPROF. The railhead and wheel surfaces were not polished or worn in the usual way. The railhead and wheels where freshly ground and machined respectively.

Figure 8 Shaft encoder and accelerometer installation: modification of axle box

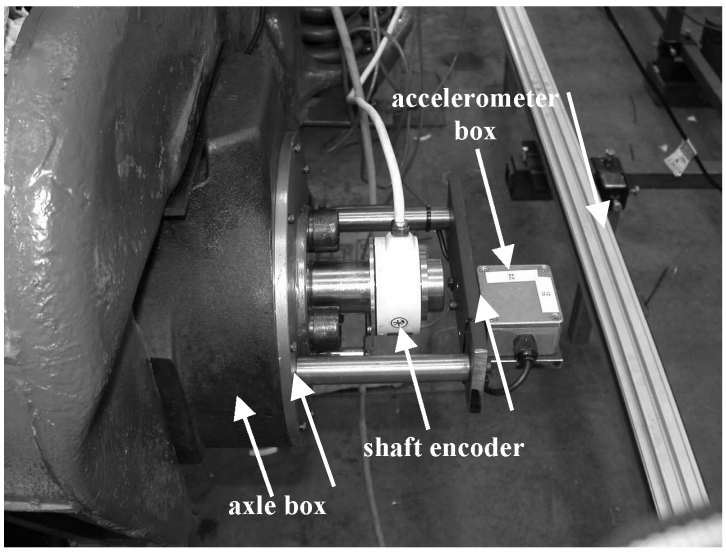

3.4 Rail friction coefficient measurement: tribometer

The friction coefficient of the rail surfaces was determined using a portable hand-pushed tribometer (product of Salient Systems). The tribometer measured the coefficient of friction at points along the rail head from the top of the running surface to the lower edge of the gauge face. The measurement was conducted by pushing the device at walking speeds to collect readings, while a proprietary algorithm reviewed the data for accuracy. The tribometer was provided by QR.

3.5 Data Acquisition (DAQ) and data analysis

A total of 18 channels of data signals were obtained and processed during the experiment. Three of them were digital signals (from two shaft encoders and one linear encoder), and the rest of 15 channels were analogue signals. These different types of the data streams were synchronised with time (computer clock) during the experiment. For this purpose a Data Acquisition (DAQ) program was developed in Lab View software platform. The program was then installed into the DAQ computer mounted on the bogie. The output of the DAQ program was provided in two binary files (one for analogue data stream and the other for digital data stream), which were then converted and merged into one data text file. To analyse the result, a program in Matlab platform was coded. The program read the data text file and plotted the data as required.

3.6 Brake controller

A pneumatic system was installed on the bogie to control the application of the brake force. Experimental conditions did not allow human control of the brakes. Also no external control-like radio link or other network interaction was available. The pressure supplied to the brake actuators was set up using the pressure regulator while the application time was adjusted using a flow restriction valve.

To control the event of braking, a solenoid valve that opened the air pressure line to the brake actuators when the electric circuit was de-energised was used. De-energising of the electric circuit at certain positions on the track was controlled automatically by the DAQ computer system. The operator of the experiment was required to just input the distance at which the brake was required to be applied; the DAQ computer system recorded this value and then compared it with the data received from the measurement of the longitudinal movement of the bogie provided by the LIMES system. This process was performed in real time during the test execution. To deal with any un-anticipated failure in the DAQ computer, a switch was designed and installed so that it could be simply disengaged (cut-off the electric circuit) by pulling a plug connected to a string.

3.7 Complete test setup

Figure 9 shows the fully instrumented bogie with its DAQ system ready for commissioning. Prior to each test trial, the DAQ was supplied with the information on the required brake pressure and the start time and rate of application of brake pressure. A road truck was used to provide the traction.

Figure 9 Instrumented Bogie with DAQ ready for commissioning

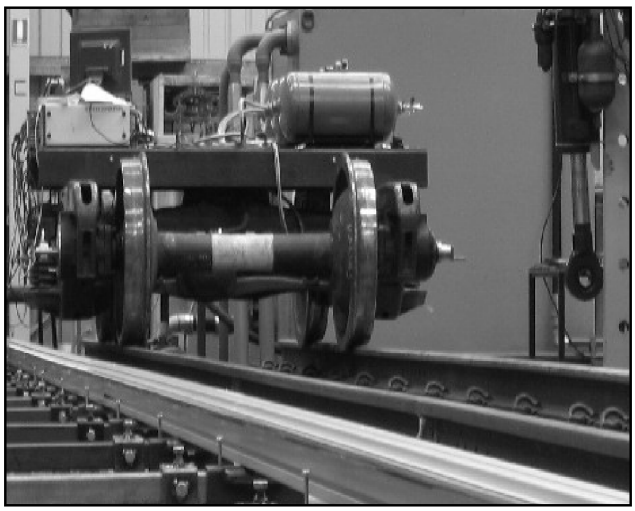

4 Results

Two cases of the bogie brake dynamics experiments were selected (Table 1). For each case the brake application time was set as 0.8 second.

Table 1 Cases of the experiment

Case	*Brake pressure* (kPa)
Case #1	130
Case #2	180

This section describes the primary and derived data obtained from each case of the experimental program.

The primary data included:

- brake normal forces (kN); from the strain gauged brake rod
- tangential brake forces (kN); from the strain gauged brake beam hanger
- accelerations (m/s^2) in the three directions; from accelerometers
- linear distance travelled (m); from the LIMES linear encoder
- angular revolution (rad); from the HENGSTLER shaft encoders.

The derived data included:

- brake torque; calculated from the tangential brake force
- longitudinal speed profile (m/s); first derivative of the LIMES data
- angular velocity (rad/s); first derivative of the HENGSTLER data
- longitudinal acceleration (m/s^2); second derivative of the LIMES data
- slip.

Where possible the derived data were compared with the measured primary data.

5 Case #1 (P = 130 kPa)

Four trials were executed where the brake cylinder pressure was controlled to reach 130 kPa maximum within 0.8 second.

5.1 Primary data

5.1.1 Brake cylinder forces: normal and tangential

Figure 10 presents the brake cylinder pressure and forces measured in the brake rods of each cylinder for trials 1–4. As can be seen in the figure, the pressure in the brake cylinder increased gradually from 0 kPa to 130 kPa in 0.8 second. The forces in the brake rods also increased gradually from zero to maximum during the corresponding period without any time lag. Both rods measured approximately the same magnitude of brake shoe normal forces. Relative to the specification of the new bogie, the measured force in the rods was approximately 18% lower, which was considered acceptable consistent with the age of the bogie.

Figure 10 Brake cylinder pressure and normal forces in the brake rods, Case #1

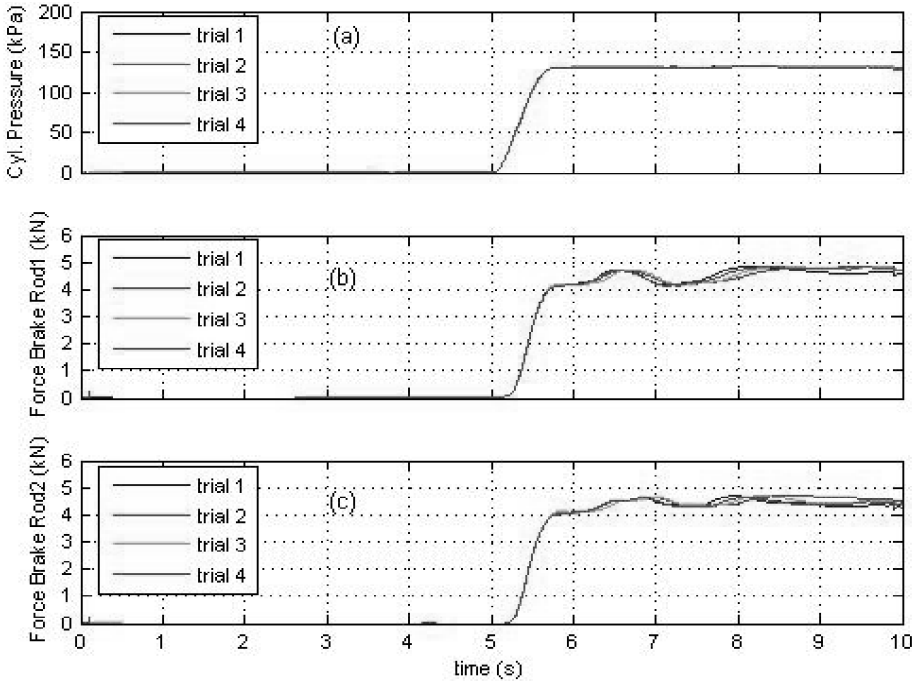

Figure 11 shows the tangential brake force measured from the brake beam hanger for trials 1–4. From the relation between the normal and tangential brake shoe forces (F_T and F_B), $F_t = \mu_b F_b$, the friction coefficient between the brake shoe and the wheel tread (μ_b) was calculated; the calculated values varied between 0.27 and 0.33.

Figure 11 Tangential brake force in the brake beam hangers, Case #1

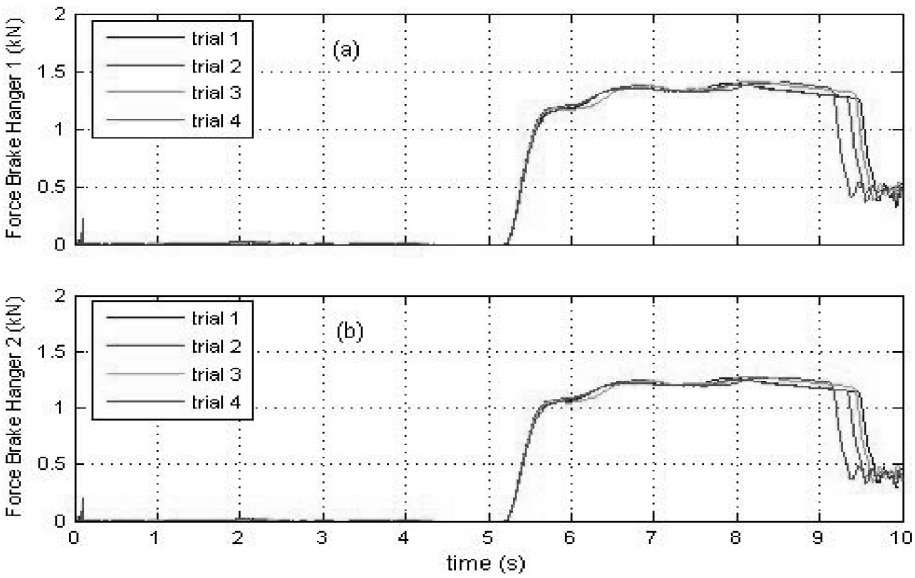

5.1.2 Accelerations: longitudinal, lateral and vertical

During the experiment, the longitudinal, the lateral and the vertical accelerations were measured using the accelerometers fitted to the axle boxes. The average of the measured longitudinal acceleration obtained from four accelerometers exhibited very good consistency amongst the four trials although each trial was conducted *without* any assurance of repeatability (Figure 12). A 16% variation of the maximum values of the longitudinal acceleration (from 2.4 m/s^2 to 2.8 m/s^2) has resulted between trials, which is considered not very significant. In the coasting zone each trial has provided very consistent acceleration (a deceleration of approximately 0.1 m/s^2). In the braking zone (the zone of interest of this test program) where the controlled brake was applied, the deceleration obtained from each trial remained relatively the same (approximately 0.75 m/s^2). Therefore the cost-effective means of accelerating the bogie was considered technically sound and satisfactory for the purpose of the investigation considered in this paper.

Figure 12 Longitudinal accelerations measured by accelerometers, Case #1

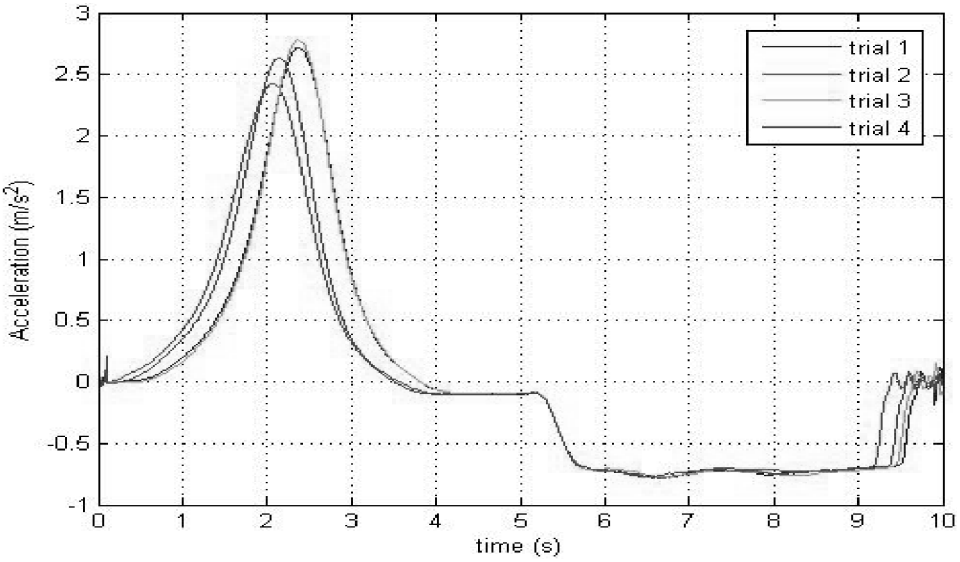

The magnitude of the lateral (average of two measurements, maximum 0.062 m/s^2) and the vertical (average of four measurements, maximum 0.048 m/s^2) accelerations measured using the accelerometers was very small both in absolute term and relative to the longitudinal acceleration. The low magnitude could be regarded as an indication of the good control exercised in each trial especially the precision of the applied pull without any lateral shift; it also reflected on the smoothness of the track, in particular the top surface of the rail. Both cases of the experiment can, therefore, be regarded as pure longitudinal dynamics investigation.

5.1.3 Linear distance travelled and angular revolution of wheelsets

The linear distance travelled and the angular revolution of the leading and the trailing wheelsets of the bogie along the test track are shown in Figure 13.

Figure 13 Travel distance and rotation of wheelsets, Case #1

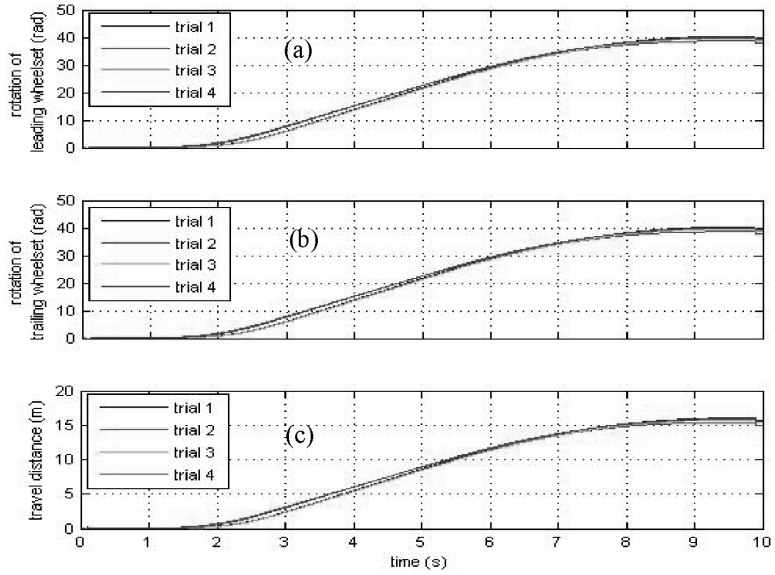

This longest travel distance was approximately 16 m. During this travel, the wheelsets rotated approximately 40 rad, or just more than six full rotations.

5.2 Derived data

5.2.1 Brake torque

Brake torque applied to the trailing wheelset was calculated using equation (1):

$$T_B = (F_{T1} + F_{T2})r_w \tag{1}$$

where T_B denotes the brake torque, F_{T1} and F_{T2} are the tangential force measured in hangers 1 and 2 respectively and r_w is the nominal radius of the wheels. The calculated brake torque time series is shown in the Figure 14.

Figure 14 Brake torques applied to the trailing wheelset, Case #1

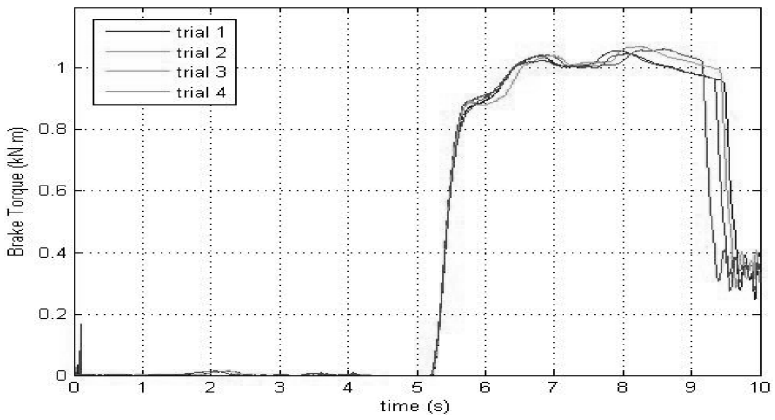

5.2.2 Speed profile and angular velocity of the wheelset

Figure 15 shows the bogie speed profile and the angular velocities of the wheelsets. The bogie speed profile is the first derivative of the dataset obtained by the LIMES linear encoder with respect to time whilst the angular velocities of the wheelsets were obtained from the first derivatives of the HENGSTLER shaft encoder datasets. From Figure 15, we can see that no skid has happened at the braked trailing wheelset for all four trials as its angular velocity is reduced to zero at the same rate as the bogie speed and the angular velocity of the non-braked leading wheelset. The maximum speed obtained was 3.14 m/s (trial 1), which was lower than the 4 m/s maximum speed for which the experiment was designed. Knowing the nominal wheel diameter, the maximum angular velocity was calculated as 7.89 m/s. The measured maximum angular velocity was 7.90 rad/s, showing the precision of the measurement system.

Figure 15 Speed profile and wheelsets angular velocity, Case #1

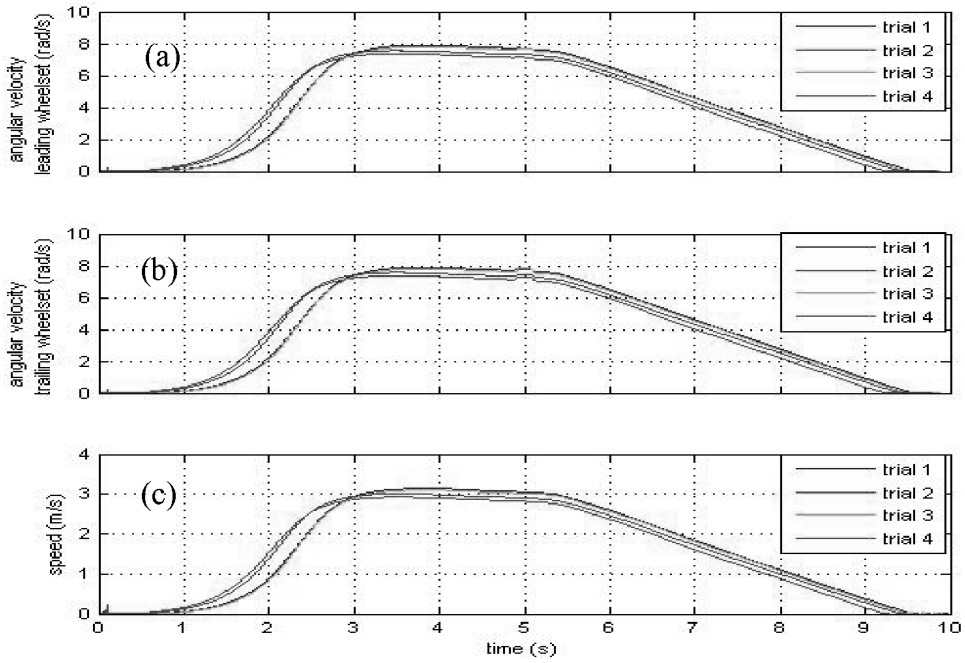

5.2.3 Longitudinal accelerations

Figure 16 exhibits the bogie longitudinal acceleration calculated through the second order numerical differentiation of the linear distance data obtained from the LIMES linear encoder. It provides a very good agreement with the direct measurement of longitudinal acceleration using accelerometers (Figure 12).

Figure 16 Accelerations calculated using linear encoder dataset, Case #1

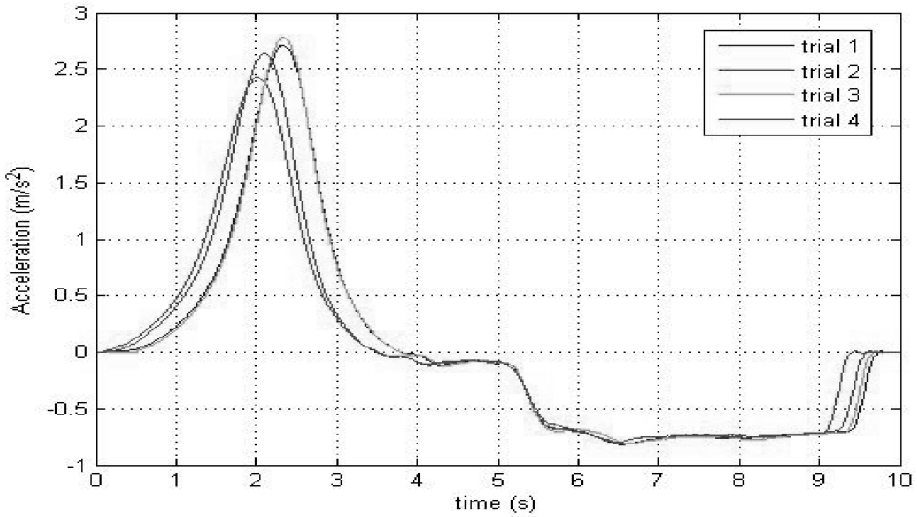

5.2.4 Slip

Due to the application of the brake, slip occurred in the contact patch of the trailing wheelset (where brake was applied). The slip was measured as the difference between the longitudinal velocity (Figure 15(c)) and the circumferential velocity of the braked wheelset (Figure 15(b)). The occurrence of slip generated a longitudinal retarding force that stopped the bogie. Figure 17 shows the difference between the longitudinal velocity and the circumferential velocity of the braked wheelset in the braking zone (from $t = 5$ s to $t = 10$ s). This figure indirectly represents the slip that occurred during the brake application.

Figure 17 Difference between the longitudinal velocity (calculate from LIMES) and the circumferential velocity of the braked wheelset, Case #1

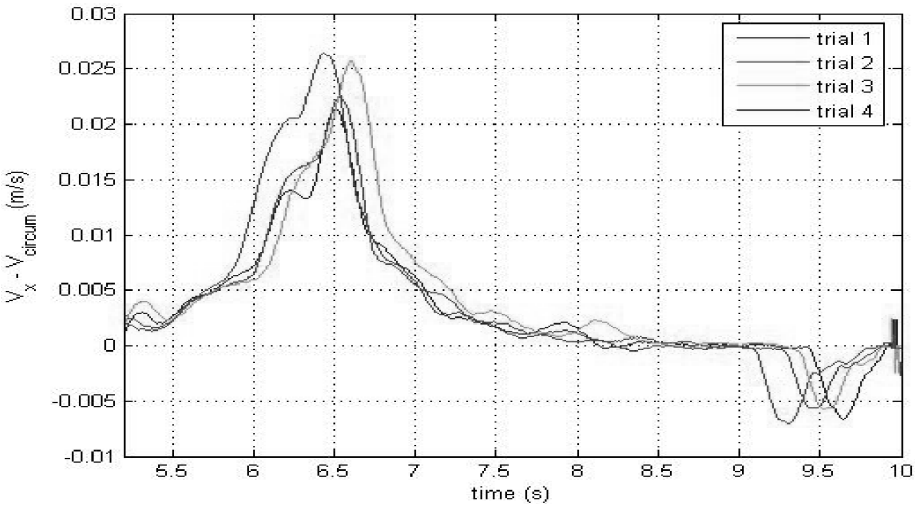

With a view to obtaining slip through another data set (namely the velocity difference of the braked and unbraked wheelsets), the reference longitudinal velocity was set equal to the circumferential velocity of the unbraked leading wheelset. The slip calculated using this method is shown in Figure 18. Both Figures 17 and 18 show very good agreement. This finding has practical significance as it appears possible to measure slip in the field without using the LIMES linear encoder system and purely through measurement of angular revolutions of the braked and unbraked wheelsets.

Figure 18 Difference between the longitudinal velocity (calculated from angular revolution of unbraked wheeslet) and the circumferential velocity of the braked wheelset, Case #1

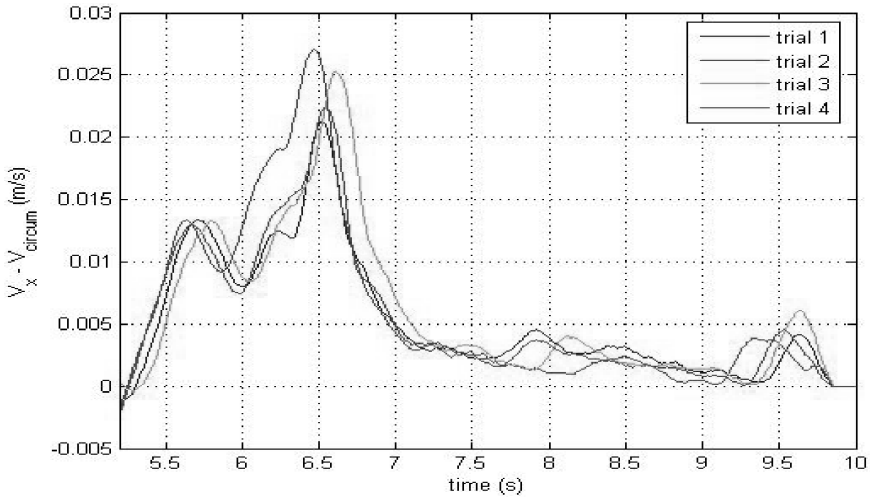

6 Case #2 (P = 180 kPa)

The purpose of the experiment Case #2 was to study the severe skid during heavy braking. In the experiment Case #2 the brake pressure was increased to 180 kPa, much above the skid limit pressure. The brake application was maintained at 0.8 second. All trials exhibited skid of the braked wheelset. Results are presented below.

6.1 Primary data

6.1.1 Brake cylinder force: normal and tangential

Figure 19 shows the brake cylinder pressure and forces measured in the brake rods of each cylinder for trials 1–4 during the execution of test Case #2. As can be seen in the figure, when the brake was applied the pressure in the brake cylinder increased from 0 kPa to 180 kPa in 0.8 second with the corresponding increase in the forces of the brake rods without any time lag. Both rods measured approximately the same magnitude of brake shoe normal forces. Similar to Case #1, the measured forces are slightly (approximately 15%) lower than that of the force specified for the new bogie due to efficiency loss of the refurbished brake cylinder.

Figure 19 Brake cylinder pressure and forces in the brake rods, Case #2

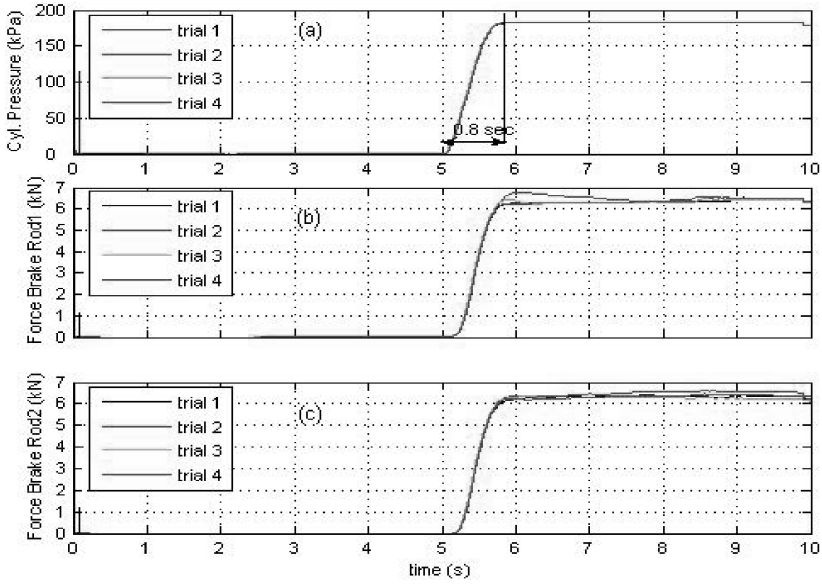

Figure 20 shows the tangential brake force measured in the brake beam hanger for trials 1–4. As both the normal and the tangential brake shoe force were measured, the friction coefficient between brake shoe and wheel tread (μ_b) was calculated. The calculated values for Case #2 varied between 0.21 and 0.28. It appears that with the increase in brake normal force, the friction coefficient reduces.

Figure 20 Tangential brake force in the brake beam hangers, Case #2

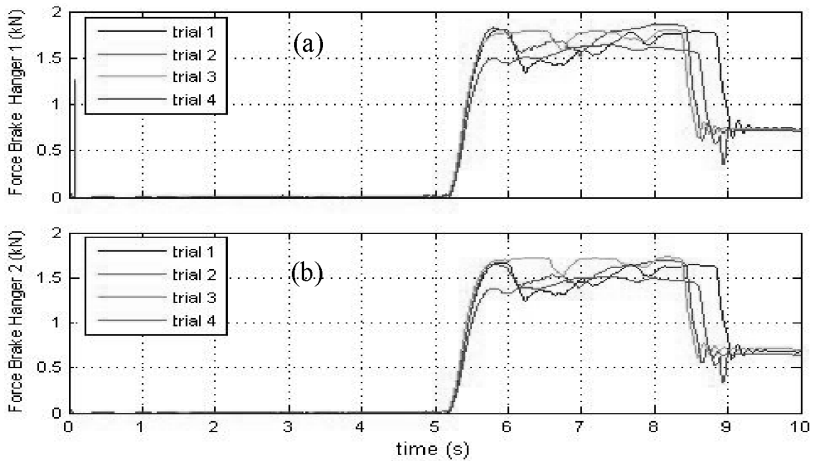

6.1.2 Accelerations

Figure 21 shows the measured longitudinal acceleration of Case #2 (average value of four accelerometers). The maximum longitudinal acceleration recorded varied from 2.2 m/s^2 to 2.5 m/s^2. Similar to the experiments in Case #1, in the coasting zone each trial

has provided a deceleration of approximately 0.1 m/s^2 due to rolling resistance. In the braking zone (the zone of interest of this test program) where the controlled brake was applied, the maximum deceleration recorded was 1.1 m/s^2 (trials 2 and 4). However, at the time of the skid, the deceleration fell to 0.5 m/s^2 (trials 1 and 2).

Figure 21 Acceleration measured by accelerometers, Case #2

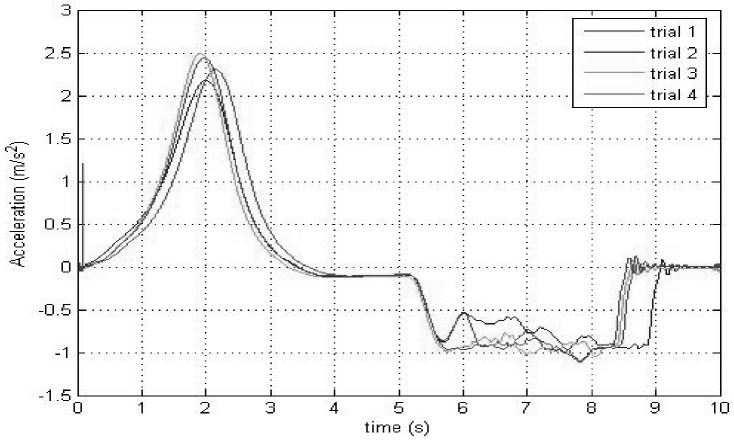

6.1.3 Linear distance travelled and angular revolutions of wheelsets

Figure 22 shows the angular revolution and the travel distance of the bogie obtained during Case #2. The maximum travel distance recorded was 16 m. Figure 22(a) and (b) reveal that for all trials the angular revolution of the braked trailing wheelset was smaller than that of the unbraked leading wheelset due to skid.

Figure 22 Travel distance and wheelsets rotation, Case #2

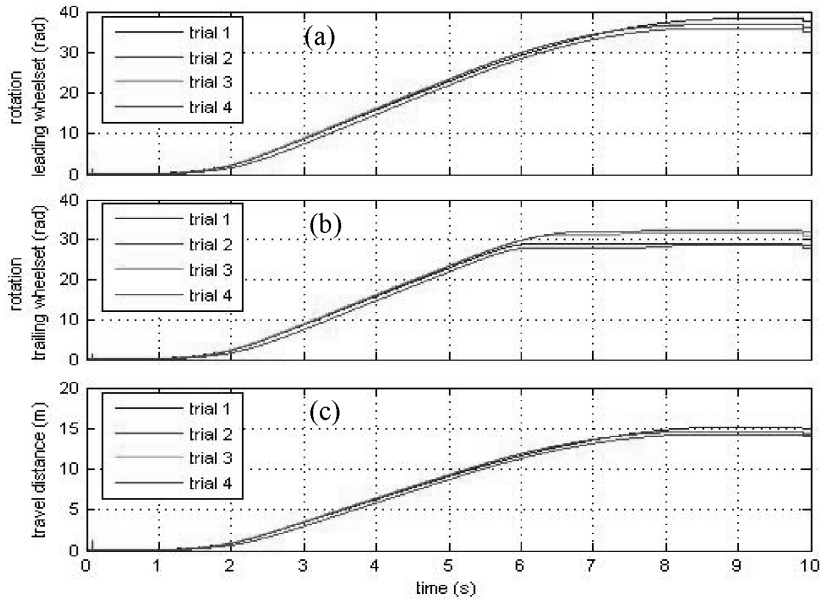

6.2 Derived data

6.2.1 Brake torque

Figure 23 shows the brake torque applied to the trailing wheelset during the experiment Case #2, calculated using equation (1). As expected, due to the skid of the trailing wheelset, the brake torque was found to drop drastically. As the most severe skid happened during trials 1 and 2, the most sudden decrease of the brake torque also occurred during these two trials. This result, again, shows that skid has significant negative effect on the braking performance.

Figure 23 Brake torques applied to trailing wheelset, Case #2

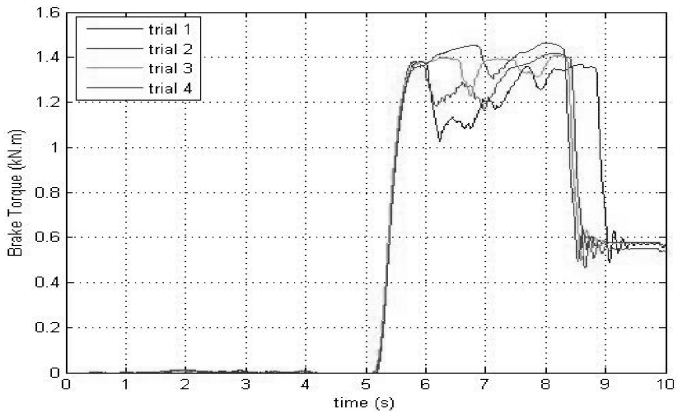

6.2.2 Speed profile

Figure 24 shows the speed profile and wheelset angular velocity during the experiment Case #2.

Figure 24 Speed profile and wheelsets angular velocity, Case #2

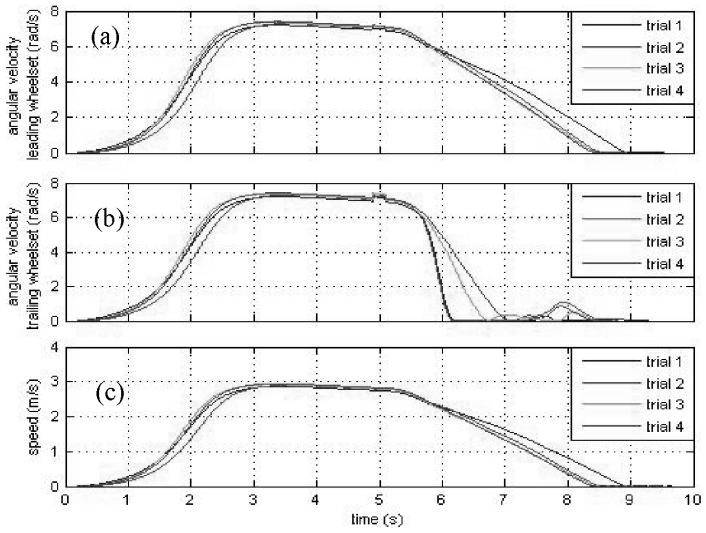

6.2.3 Longitudinal acceleration

Figure 25 exhibits the bogie longitudinal acceleration time series obtained during the experiment Case #2, calculated through second order numerical differentiation of the linear distance data obtained from the LIMES linear encoder. Similar to the experiments in Case #1, it provides a very good agreement with the direct measurement of longitudinal acceleration using accelerometers.

Figure 25 Longitudinal acceleration calculated from LIMES, Case #2

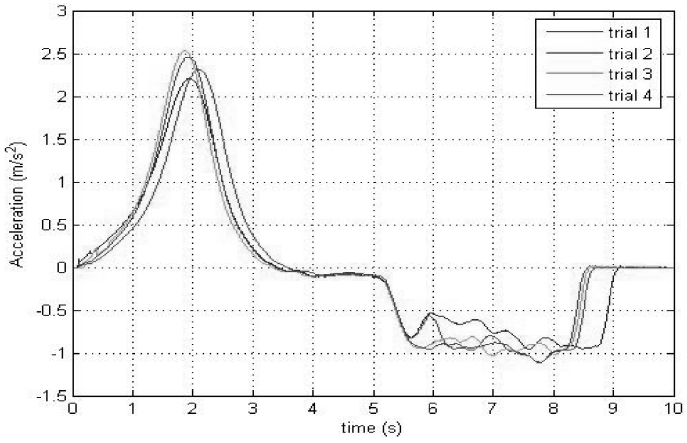

6.2.4 Slip

The slip that occurred during the brake application of Case #2 is shown in Figures 26 and 27. The longitudinal velocity was used to obtain the curves in Figure 26 whilst the angular revolution of the unbraked wheelset was used to obtain the curves in Figure 27. Both figures show very good agreement. For trials 1 and 2 the skid was detected at around 2.2 m/s, and for trials 3 and 4 it was detected at lower speeds of 1.65 m/s and 1.35 m/s respectively.

Figure 26 Difference between the longitudinal velocity (calculated from LIMES) and the circumferential velocity of the braked wheelset, Case #2

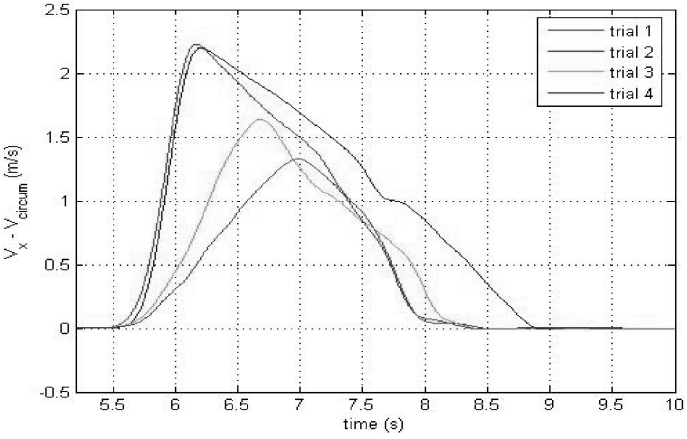

Figure 27 Difference between the longitudinal velocity (calculated from angular revolution of unbraked wheelset) and the circumferential velocity of the braked wheelset, Case #2

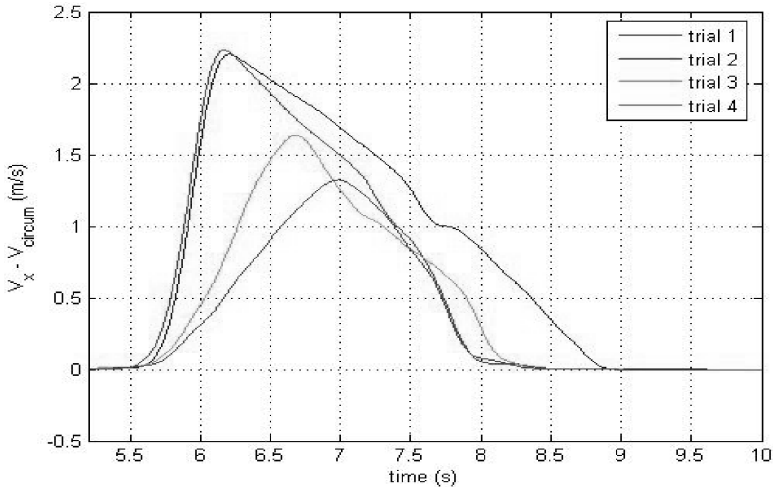

6.3 Friction coefficient between the wheel and the rail

When skid occurs the following equation is fulfilled:

$$T_B = (\mu_{r1} N_{w1} r_{w1}) + (\mu_{r2} N_{w2} r_{w2}) \tag{2}$$

where T_B is the brake torque applied to the wheelset (see equation (1)), μ_{r1} and μ_{r2} are the friction coefficients at the right and the left wheel-rail contact patches respectively, N_{w1} and N_{w2} are the normal loads on the right and the left wheel-rail contact patches respectively and r_{w1} and r_{w2} are the rolling radius of the right and the left wheels respectively. Assuming $\mu_{r1} \approx \mu_{r2} = \mu_r$ and rolling radius of the wheels $r_{w1} \approx r_{w2} = r_w$, equation (2) can be written as

$$T_B = \mu_r r_w (N_{w1} + N_{w2}). \tag{3}$$

During the experiments T_B was obtained by measuring the tangential brake force whilst the nominal wheel radius $r_w = 0.398$ m, measured prior to the test execution and N_{w1} and N_{w2} were the right and the left wheel load (sum of the components due to static load and bogie pitching dynamics) of the braked wheelset respectively ($N_{w1} \approx N_{w2} \approx 8.85$ kN). Therefore, when skid happened, the friction coefficient between wheel and rail, μ_r, was calculated using equation (3).

The calculated friction coefficient between the wheel and the rail during the occurrence of skid in this experiment program was found to vary between 0.15 and 0.20. The low coefficient is believed to be typical of 'rough' running surfaces; as the running surfaces were not polished to any precision and patches of corrosion products were visible to the naked eye, especially on the railhead, the low friction was considered acceptable.

The friction coefficient calculated from the skid measurements was much lower than the value obtained from the tribometer measurement (0.50–0.55 for dry rail and 0.43–0.46 for rail lubricated with soap solution). As tribometer measurements could not be regarded as an accurate reflection of the actual case (due to speed/wheel profile/wheel material, for example), the measured tribometer values were disregarded. Field practice also agrees with this decision as tribometer values are only used to determine *relative* changes to the friction coefficients rather than for the *absolute* measure. The friction coefficient calculated from equation (2) is considered appropriate for usage in simulations.

7 Summary and conclusion

An experimental program was designed and commissioned with the primary objective of investigating the influence of braking torques to the longitudinal dynamics of bogies, in particular to calculate the speed profile and the corresponding wheelset pitch due to the application of braking torque. In the experiment a fully controlled and measured brake force was applied to the trailing (rear) wheelset of the bogie. Measurement devices were carefully chosen to meet the requirement of high precision data. The mounting details for each of the devices were carefully designed so that the data could be gathered accurately.

All measurement devices (both onboard and wayside) worked well giving accurate results resulting in good inter-dependent comparisons. All the data gathered from the measurements were found to be consistent. Two cases of experiments were selected for the purpose of reporting. The only variable between the three cases was the brake pressure (130 kPa and 180 kPa) with the brake application time being kept constant (0.8 second) for all cases. From a practical perspective, these pressures are found to generate very high brake severity expressed in terms of BFR of 52% and 72% respectively.

From the results of the experiments some important conclusions can be drawn as listed below:

- The piston forces exerted by the brake cylinder (force measured in brake rod) were found to be approximately 15–18% lower than the value calculated from the bogie specification at its new condition indicating reduction in the efficiency of the refurbished bogie brake system.
- At the brake pressure of 130 kPa no skid was detected. At the brake pressure of 180 kPa, wheelset skid was detected for all the four trials.
- The acceleration signatures obtained from direct measurement using the accelerometers agree very well with the acceleration signatures calculated from the second order numerical difference of the LIMES linear encoder data set.
- Both slip calculations using LIMES linear encoder and using non-braked wheelset shaft encoder as reference to calculate longitudinal velocity showed very good agreement. This finding leads to potential field measurement of slip *without* the LIMES linear encoder.

- From the measurement of the normal and tangential brake shoe forces, friction coefficients between the brake shoe and the wheel tread were calculated for all cases. It appeared that with the increase in brake shoe forces (or brake cylinder pressure), the coefficient of friction between the brake shoe and the wheel tread reduces. For the 130 kPa and 180 kPa cylinder pressures, the average friction coefficients determined were 0.30 and 0.25 respectively. (A 150 kPa case was also studied – but not reported, which provided an average value of friction coefficient of 0.27). This indicates that there is a tendency for the friction coefficient to reduce with the increase in brake pressure.
- From the four skid trials reported in this chapter, the friction coefficient between the wheel tread and railhead was determined and was found to vary between 0.15–0.20. This range is much smaller than the coefficients determined from the tribometer readings (0.50–0.55). As the tribometer is considered more relevant for understanding relative changes in friction coefficient, the absolute values of friction coefficient obtained from the tribometer measurements were disregarded. The more reliable determination of friction coefficient between the wheel tread and railhead is therefore considered to be the one obtained through the skid trials (0.15–0.20).

Acknowledgements

The support and involvement of Andrew Nelmes and Bruce Brymer (both QR), Florian Sumpf (Aachen, Germany), Bernard Jansen, Gary Hoare, Ian Major, Grant Caynes, Trevor Ashman, Chris Bossomworth (All CRE, CQU), and innumerable staff of QR involved in the design and commissioning of the experimental program is gratefully acknowledged. The CRE and INKA Indonesia funded the project.

References

Andrews, H.I. (1986) *Railway Traction; The Principles of Mechanical and Electrical Railway Traction*, Elsevier Science Publisher, Netherlands.

Balas, M., Balas, V., Foulloy, L. and Galichet, S. (2001) 'A model of the sliding wheel during braking', *5th International Conference on Railway Bogies and Running Gear*, Budapest.

Berghuvud, A. (2002) 'Freight car curving performance in braked condition', *Journal of Rail and Rapid Transit*, Vol. 216, pp.23–29.

Carter, F.W. (1926) 'On the action of a locomotive driving wheel', *Proc. Royal Soc. Ser.*, Vol. A112, pp.151–157.

Dukkipati, R.V. (2000) *Vehicle Dynamics*, CRC Press, Boca Raton, Fla.

Lixin, Q. and Haitao, C. (2001) 'Three dimension dynamics response of car in heavy haul train during braking mode', *7th International Heavy Haul Conference*, Brisbane, Australia.

Olson, B.J. (2001) *Nonlinear Dynamics of Longitudinal Ground Vehicle Traction*, Mechanical Engineering, Michigan State University, Michigan, USA.

Polach, O. (1999) *A Fast Wheel-Rail Forces Calculation Computer Code*, Vehicle System Dynamic Supplement, Vol. 33, pp.728–739.

Polach, O. (2005) 'Creep forces in simulation of traction vehicles running on adhesion limit', *Wear*, Vol. 258, pp.992–1000.